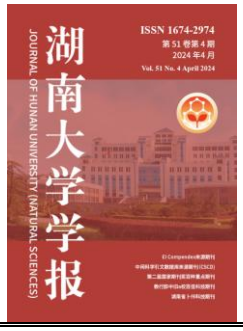

湖南大学学报（自然科学版）
Journal of Hunan University (Natural Sciences)

第 51 卷 第 4 期
2024 年 4 月

Available online at http://jonuns.com/index.php/journal/index

Vol. 51 No. 4
April 2024

Open Access Article

https://doi.org/10.55463/issn.1674-2974.51.4.6

Heat Transfer Enhancement and Pumping Power Characteristics of Fe_2O_3 and ZnO Nanofluids in a Double-Pipe Heat Exchanger

Azhar Hussain Shah[1], Waqar Ahmed[2], Liaquat Ali Memon[1], Abdul Ghaffar[3], Muhammad Ramzan Luhur[1], Qadir Buksh Jamali[1], Umair Ahmed Rajput[1]*

[1] Department of Mechanical Engineering, Quaid-e-Awam University of Engineering Science & Technology, Nawabshah, 67480, Sindh, Pakistan

[2] Institute of Turbomachinery, School of Energy and Power Engineering, Xi'an Jiaotong University, Xi'an, 710049, China

[3] Engineering Institute of Technology, Melbourne, VIC 3000, Australia

* Corresponding author: engr.umair@quest.edu.pk

Received: January 19, 2024 / Revised: February 4, 2024 / Accepted: March 9, 2024 / Published: April 30, 2024

Abstract: Engineered colloidal suspensions of nanoparticles in base fluids such as water, ethylene glycol, and propylene glycol constitute nanofluids (NFs). Typically, metals, oxides, carbides, and carbon nanotubes are the nanoparticles employed in NFs. NFs possess distinctive properties that offer potential advantages in various heat transfer applications, including fuel cells, hybrid-powered engines, microelectronics, and pharmaceutical processes. The convective heat transfer coefficient and thermal conductivity of NFs are higher than those of base fluids. This study delves into the potential performance in heat transfer rate and fluid flow characteristics, specifically pumping power, on a double-pipe heat exchanger using baseline water, iron oxide, and zinc oxide NFs at volume concentrations ranging from 0.10% to 0.175% under a flow regime of 1700 to 3400. In this study, the NF and hot fluid (hot oil) were moved in parallel- and counter-flow directions at flow rates of 1, 1.25, 1.5, and 2 (1.6×10^{-5} to 3.3×10^{-5} m^3/sec) to determine the behavior of baseline water and NF when oil was heated at 60°C. The main purpose of this investigation is to determine the maximum heat transfer rate from hot oil to cold fluid using zinc oxide NF, iron oxide NF, and baseline water. In this study, maximum heat was transferred from hot oil to cold fluid at various flow rates for zinc oxide NF compared with iron oxide NF and baseline water. The purpose of this study was to experimentally examine the heat transfer rate and fluid flow characteristics, specifically focusing on pumping power, of a double-pipe heat exchanger, utilizing baseline water, iron oxide, and zinc oxide NFs in the heat exchanger, with a fixed inlet temperature of 60°C for the hydraulic oil. The enhancements in the heat transfer coefficient, the Reynolds number, friction factor, and pumping power were also investigated under laminar and turbulent flow regimes. The results showed that the heat transfer coefficient, friction factor, and pumping power of Fe_2O_3 and ZnO NFs are slightly greater than those of baseline water at volume concentrations of 0.100, 0.125, 0.150, and 0.175%. At any given volume concentration, the ZnO NF showed a higher heat transfer coefficient than Fe_2O_3 NF and baseline water because the thermal conductivity of the ZnO NF is higher than that of both fluids. However, pumping power is consumed more using Fe_2O_3 NF in both types of heat exchangers than other fluids because of its higher density. Based on this study, heat is transferred between hydraulic oil ISO VG 64 (hot fluid) and baseline water (cold fluid), while in previous studies, heat was supposed only transferred between hot and cold water due to their applications. This study also focuses on addressing the challenges encountered by large mechanical equipment bearings, such as overloading and overheating. To address these conditions, the oil was processed and directed toward a double-pipe heat exchanger to efficiently transfer its heat to Fe_2O_3 and ZnO NFs. The results suggest that the ZnO NF could function very well as a working fluid for industrial requirements compared with other NFs and conventional baseline water.

Keywords: heat transfer, heat exchanger, nanofluid, volume concentration, Fe_2O_3, ZnO.

双管换热器中氧化铁 和氧化锌纳米流体的传热强化和泵送功率特性

摘要：纳米流体(NF)是由纳米颗粒在水、乙二醇和丙二醇等基础流体中形成的工程胶体悬浮液。通常，金属、氧化物、碳化物和碳纳米管是NF中使用的纳米颗粒。NF具有独特的特性，可在各种传热应用中提供潜在优势，包括燃料电池、混合动力发动机、微电子和制药工艺。NF的对流传热系数和热导率高于基础流体。本研究深入研究了使用基准水、氧化铁和氧化锌NF（体积浓度范围为0.10%至0.175%）在1700至3400的流动状态下，双管热交换器的潜在传热速率和流体流动特性（特别是泵送功率）性能。在本研究中，NF和热流体（热油）以1、1.25、1.5和2（1.6×10-5至3.3×10-5立方米/秒）的流速沿平行和逆流方向移动，以确定油在60摄氏度加热时基准水和NF的行为。本研究的主要目的是确定使用氧化锌NF、氧化铁NF和基准水时从热油到冷流体的最大传热速率。在本研究中，与氧化铁NF和基准水相比，氧化锌NF在不同流速下将最大热量从热油传递到冷流体。本研究的目的是通过实验检查双管热交换器的传热速率和流体流动特性，特别是泵送功率，热交换器中使用基准水、氧化铁和氧化锌NF，液压油的入口温度固定为60摄氏度。在层流和湍流状态下，还研究了传热系数、雷诺数、摩擦系数和泵送功率的增强。结果表明，在体积浓度为0.100、0.125、0.150和0.175%时，氧化铁和氧化锌NF的传热系数、摩擦系数和泵送功率略高于基准水。在任何给定的体积浓度下，氧化锌NF显示出比氧化铁NF和基准水更高的传热系数，因为氧化锌NF的热导率高于这两种流体。然而，由于氧化铁NF的密度较大，因此在这两种类型的热交换器中使用时，泵送功率比其他流体消耗更多。根据这项研究，热量在液压油ISO VG 64（热流体）和基准水（冷流体）之间传递，而在之前的研究中，由于它们的应用，热量被认为仅在热水和冷水之间传递。这项研究还侧重于解决大型机械设备轴承遇到的挑战，例如过载和过热。为了解决这些情况，对油进行处理并引导至双管热交换器，以有效地将其热量传递给氧化铁和氧化锌NF。结果表明，与其他NF和传统基准水相比，氧化锌NF可以很好地用作满足工业要求的工作流体。

关键词：传热，热交换器，纳米流体，体积浓度，氧化铁，氧化锌。

1. Introduction

Different nanoparticles are now used to enhance various thermal properties of nanofluids (NFs), such as heat transfer rate and thermal conductivity [1-2]. The addition of nanoparticles to the base fluid increases the thermal properties of the fluid [3]. NFs have unique characteristics that could prove beneficial in various heat transfer applications such as fuel cells, hybrid-powered engines, microelectronics, and pharmaceutical processes. The convective heat transfer coefficient and thermal conductivity of NFs are higher than those of base fluids. Sunil Kumar et al. carried out their research on the thermal characteristics of zinc oxide/water/ethylene glycol NF in a square duct. The results revealed that the heat transfer coefficient is increased in the square duct, which is 3.1 times greater than that in the other ducts [4]. Gnanavel et al. focused on the thermal performance of zinc oxide within a rectangular twisted tape heat exchanger, analyzing its effectiveness in transitioning from laminar to turbulent flow. They compared the results with those of other fluids and concluded that zinc oxide exhibits superior heat flow characteristics [5]. Stephan et al. showed the impacts of nanosized particles, their shape, and concentration on the performance of NFs, i.e., heat transfer coefficient and pressure drop. It was also

shown that the heat transfer efficiency was increased by 30% when using metal oxide NFs, and the results were compared to those obtained with baseline water [6]. Few other researchers have used water/silica and iron oxide NFs. The Reynolds number with turbulent flow is considered to be in the range of 30,000 to 45,000 at a volume fraction of 2% to 5%. The pressure drop, performance evaluation criteria, and energy efficiency were examined. The results suggested that the water performance showed a lower value than water/silica and iron oxides [7].

Zhou et al. revealed the characteristics of NFs in the radiator of a car. Zinc oxide and aluminum oxide in various proportions were mixed with propylene glycol to obtain the NF. The result showed that a 46% enhancement in the heat transfer rate occurred at a 0.2% volume concentration of zinc oxide-propylene glycol NF [8]. Another study was conducted to investigate fouling deposition on the surface of heat exchanger tubes. It was found that the fouling factor increased because of the increase in temperature and volume concentrations [9]. This paper reveals the basic ideas of energy storage by reducing its charging time. In this investigation, the discharge time was reduced by 25% through the use of NFs. An experiment was carried out on a double-pipe heat exchanger to determine the heat transfer coefficient, friction factor, and energy losses. The friction factor was increased approximately 2.4 times in both parallel- and counter-flow heat exchangers at the Reynolds numbers 6500–13000 [10]. The investigations focused on analyzing the fluid flow and design characteristics of a heat exchanger utilizing corrugated pipes [11]. The study was conducted under a laminar flow regime using iron oxide NFs with diameters of 20 nm at a volume concentration of 0.08-01% to determine the heat transfer characteristics and Nusselt number. The results showed that heat transfer was increased about 12-26% than that of pure water base fluid [12]. Various designs of heat exchangers were used in various processing devices and locations.

2. Literature Review

2.1. Heat Exchanger Design

The design of a heat exchanger plays a vital role in determining hydrothermal characteristics. The operational parameters of the heating device were analyzed numerically under laminar flow conditions [13]. The researchers presented their work on numerical analysis and CFD. Numerical analysis was performed in a counter-flow heat exchanger using various types of metallic oxide: Al_2O_3, CuO, and TiO_2. It is revealed that the heat transfer rate was increased in NFs compared with baseline water [14]. The authors focused on the numerical study of double- and triple-pipe heat exchangers and found various fluid characteristics [15]. The objective of this study was to experimentally investigate the heat transfer characteristics of NF containing zinc oxide nanoparticles with a diameter of 30 nm. The NF demonstrated superior performance compared to water at flow rates of 2, 4, and 6 LPM [16]. The authors presented their work on various thermal characteristics using aluminum oxide, copper oxide, zinc oxide, and water in a test rig using various volume concentrations, i.e., 0.025% -0.1%. From experimental results, it was shown that titanium oxide produced better heat transfer rates than other NFs [17].

This paper aimed to prepare the best NF solution that enhances the thermal properties of the fluid on a large scale. The solution was prepared by mixing 30-nm-diameter ZnO nanoparticles in water and passing it through a heat exchanger at volume flow rates of 2, 4, and 6 LPM. Furthermore, the heat transfer characteristics are influenced by various parameters such as the shape, size, and concentration of nanoparticles [19]. Table 1 shows the thermal properties of the nanoparticles.

Table 1 Thermal properties of the nanoparticles [18]

N_p	Density (kg/m^3)	Thermal Cond. (W/m. K)	Specific heat capacity (J/kg. K)	Appearance
Iron oxide (Fe_2O_3)	8800	7	104	Radish powder
Zinc oxide (ZnO)	5600	13	667	White powder

The objectives of this study are to improve heat transfer rates and experimentally analyze the pumping power consumption. Actually, this study focuses on the use of iron oxide and zinc oxide NFs as coolants in a double-pipe heat exchanger. The goal is to analyze their performance under different flow rates and operating temperatures for both the hot and cold fluids. One of the primary factors considered in selecting this study is the potential for enhancing industrial applications through the utilization of nanoparticles in the base fluid. This approach aims to achieve superior results in both types of heat exchangers. Another criterion for selecting the objective is the thermal conductivity of nanoparticles, which can improve fluid flow characteristics, pressure drop, and pumping power.

In addition, this study delves into the stability of NFs and the methods used in their preparation. This study is applicable to industrial processing where hot and cold fluids exchange their maximum possible heat. During this investigation, heat was transferred solely from hot oil to cold NF. This unique aspect of the study sets it apart from other research in the field. Moreover, the Nusselt number was measured and calculated, then compared with the correlation equation. It was determined that the experimental and theoretical

correlations closely aligned with their respective values. A NF is a combination of nanosized particles of metals or metal oxides in the base fluid and is used in various human activities and industrial processes. This discovery has a wide range of applications, including heating processing equipment, heat exchangers, power engineering devices, the chemical industry, medicine, solar collectors, and electronic devices.

3. Research Methodology

In this study, baseline water, iron oxide (Fe_2O_3), and zinc oxide (ZnO) NFs were used as coolants in a double-pipe heat exchanger (DPHEx). The experimental test rig used in this study is shown in Fig. 1. The test section of the rig consists of two concentric tubes, each containing hot and cold fluids that flow in the counter-flow direction. Additionally, there is an oil storage tank equipped with an oil pump, a gate valve, and a ball valve (BV) for regulating the flow of the hot and cold fluids. The test section consists of a 0.91-m-length copper pipe with inner and outer diameters measuring 0.545 and 0.625 inches, respectively. To reduce the heat losses from the tubes, an insulating material is employed. Thermocouples are installed in the inlet and outlet of the hot and cold fluid pipes to measure the temperature.

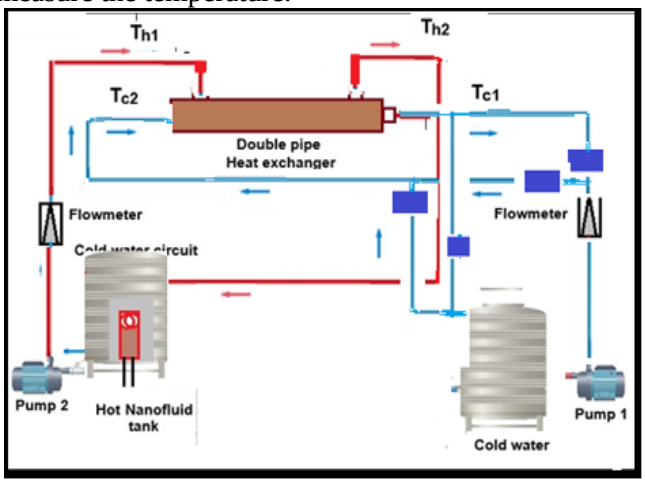

Fig. 1 Schematic of the test rig (The authors)

The storage tank is constructed from stainless steel and designed for storing cold fluid, specifically Fe_2O_3 and ZnO NF. Thus, NFs are moved through the pump toward the double-pipe heat exchanger to absorb more heat from hot fluid, i.e., hydraulic oil ISO VG 68. During the experiment, the flow rate, wall temperature of the test rig, and inlet and outlet temperatures of hot and cold fluids were measured separately. All T-type thermocouples were calibrated using a programmable calibrator with an accuracy of ±0.1. The uncertainty of the voltmeter was also ±0.1. Moreover, the flow rates of NFs were calculated using a digital flow meter with an uncertainty of ±0.1. Upon completion of the operational testing of the test rig, measurements were taken for pressure difference, flow rate, temperature, voltage, and current using the installed devices. The readings obtained were found to be appropriate for determining the heat transfer coefficient and other thermal performance parameters. Before operating the test rig, the oil storage tank was filled with hot fluid, specifically ISO VG-68 hydraulic oil, up to the standard level. The oil was then heated at 60°C. The flow rate was controlled in the range of 1-2 LPM. Finally, samples of oil and NF were collected to measure a range of thermal properties, including viscosity, density, specific heat, and thermal conductivity of the NF. Fig. 2 shows various laboratory devices through which thermal properties, i.e., viscosity, density, and thermal conductivity of the NF, were measured separately.

Fig. 2 Measuring devices (The authors)

3.1. Sample Preparation and Measurements

A NF is a balanced mixture of Fe_2O_3 and ZnO nanoparticles suspended in baseline water. The NF was created by dispersing iron oxide (Fe_2O_3) and zinc oxide (ZnO) nanoparticles in baseline water, with particle sizes of 20 and 30 nm, respectively. The concentrations used were 0.100%, 0.125%, 0.150%, and 0.175% by volume. Moreover, when solid particles with high thermal conductivity are added to the baseline water, the heat transfer rate and pumping power are higher than those of the ordinary base fluid. Fig. 3 shows a flow diagram of the research methodology. Fe_2O_3 and ZnO nanoparticles in dry powder form, with average particle sizes of 20 and 30 nm, respectively, were procured from the market. The nanoparticles were mixed in baseline water at their volume concentration to create a high-quality NF solution using the standard method outlined below:

$$\phi = \frac{\left(\frac{wp}{\rho p}\right)}{\left(\frac{wp}{\rho p}\right)} + \left(\frac{wbf}{\rho bf}\right) \times 100 \qquad (1)$$

where ρp and ρbf - densities of nanoparticles and base fluid, respectively (kg/m^3), W_{bf} - weight of base fluid

(liters), and W_p - weight of nanoparticles (kg). The stability of the NF is a very essential parameter for absorbing more heat from hot fluids. Numerous methods are applied for NF stability, i.e., single-step and two-step methods. These methods are highly preferred and applied due to their higher efficiency. Moreover, in this study, the NF was prepared by mixing Fe_2O_3 and ZnO nanoparticles in a baseline using a two-step method with a concentration range of 0.10-0.175% by volume. Following this method, a stabilization process was implemented to prevent the potential agglomeration of nanoparticles in the baseline water, resulting in a highly effective suspension. The hot plate magnetic stirrer method is utilized for a continuous period of 2-3 hours to effectively blend the nanoparticles into the baseline water. It is anticipated that the NF will remain stable for an extended period, lasting at least 24 h. Thus, the stabilized NF was obtained using the two-step method and transferred to the double-pipe heat exchanger for selecting either a parallel- or counter-flow arrangement. During the final stage of the test rig process, temperatures of the hot and cold fluids were recorded. Subsequently, samples of the NF were collected. In this way, various thermal properties were measured successfully using calibrated devices.

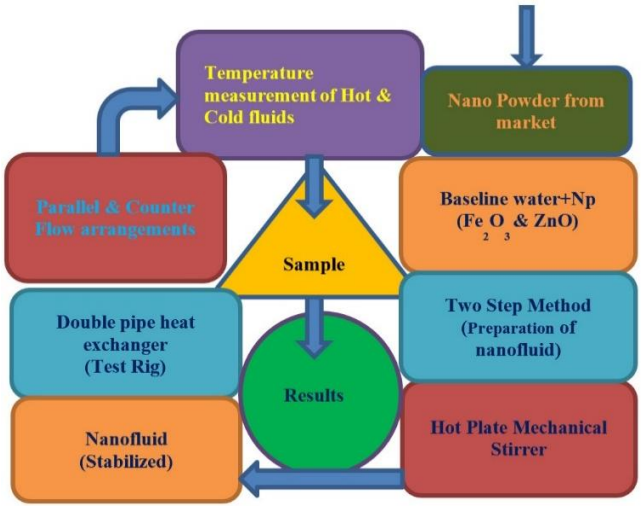

Fig. 3 Flow diagram of the research methodology (The authors)

Table 2 displays the specific positions of BVs in the double-pipe heat exchanger during operation. The table allows the selection of parallel- and counter-flow arrangements by opening or closing the BVs.

Table 2 Valves and their positions (The authors)

Valve	Parallel flow	Counter flow
BV-1	Open	Closed
BV-2	Closed	Open
BV-3	Open	Closed
BV-4	Closed	Open

$$\rho nf = \phi.\rho p + (1-\varphi)\, bf$$

where ρp and ρbf are densities of the nanoparticle and base fluid, respectively.

$$\mu nf = (1+2\varphi)\,\mu f$$

The heat was produced by heating hydraulic oil at the desired temperature within the double pipe of the heat exchanger. To maintain optimal operating conditions, it is necessary to remove or reduce this heat by circulating another fluid, such as baseline water or NF, in either the parallel- or counter-flow direction. During the contact between the surfaces of both pipes, heat was transferred from the hot fluid to the cold fluid. The rate of heat transfer from the hot fluid to the coolant is calculated as follows:

$$Qw = mw\ Cpw\,(Tin - Tout)\quad (W) \qquad (2)$$

$$Qnf = mnf\ Cpnf\,(Tin - Tout)\quad (W) \qquad (3)$$

Heat flux:

$$q'' = Q/\Pi DL\ (Watt/m2) \qquad (4)$$

where Q is the heat transfer rate in watts, D is the diameter of the pipe in meters, and L is the length of the pipe in meters.

Heat transfer coefficient:

$$h = (q'')/(Tw - Tb) \qquad (5)$$

where h is the convective heat transfer coefficient in $W/m^2.K$, Tw is the wall temperature in °C, Tb is the bulk temperature in °C.

The Nusselt number:

$$Nu = \frac{hD}{k} \qquad (6)$$

where h is the convective heat transfer coefficient in $W/m^2.K$, D is the diameter of the pipe in meters, K is the thermal conductivity of the fluid in W/m.K.

The Reynolds number:

$$Re = \frac{\rho VD}{\mu} \qquad (7)$$

where ρ is density of the fluid in Kg/m^3, V is velocity of the fluid, D is the diameter of the pipe in meters, and μ is dynamic viscosity of the fluid in Pa.sec. The correlation equations developed by Pak and Cho et al. [19] can be utilized to estimate thermal properties of NFs.

Density of the NFs:

(8)

Effective viscosity of the NFs:

(9)

where μf is dynamic viscosity of the NF in Pa.sec, and φ is the volume concentration of np in %.

Pumping power:

$$\frac{W_{nf}}{W_{bf}} = (\frac{\mu_{nf}}{\mu_{bf}})^{0.25}.(\frac{\rho_{nf}}{\rho_{bf}})^{2} \quad (10)$$

where μ_{nf} is dynamic viscosity of the NF in Pa.sec, and ρ_{nf} is the density of the NF in kg/m^3.

4. Results and Discussion

4.1. Density and Viscosity of Fe_2O_3 and ZnO NFs

The addition of Iron oxide (Fe_2O_3) and zinc oxide (ZnO) nanoparticles to the baseline water resulted in an increase in the density of both fluids. The density of Fe_2O_3 NF is greater than that of ZnO NF because the density of iron oxide is higher than that of zinc oxide at the same operating temperatures. The density of both NFs was measured using a pycnometer. The results obtained can be compared with correlation equation (8), revealing a strong agreement between theoretical and experimental results for Fe_2O_3 and ZnO NFs at volume concentrations of 0.100%, 0.125%, 0.150%, and 0.175%. The density of the baseline water increased with the addition of nanoparticles, as demonstrated by the notable increment in densities. This increase in densities is illustrated in Fig. 4. The maximum increment from iron oxide is recorded as 1033 kg/m^3, making it denser than other fluids.

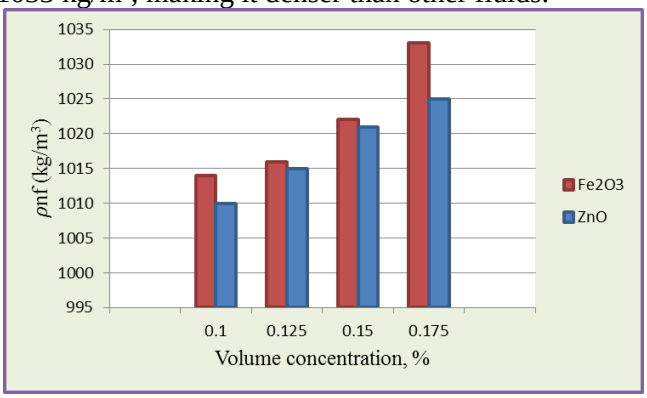

Fig. 4 Density of Fe_2O_3 and ZnO NFs at various volume concentrations (The authors)

Density is a crucial factor in the calculation of heat transfer. The density of NF varies with changes in temperature. As the temperature rises, the density of both fluids decreases, as illustrated in Fig. 5. It is shown that the density and thickness of Fe_2O_3 and ZnO NFs decrease continuously due to continuous heating.

The mixture of Fe_2O_3 and ZnO nanoparticles in baseline water at concentrations ranging from 0.10% to 0.175% resulted in increased viscosity compared to baseline water. Thus, a higher viscosity was observed in the Fe2O3 NF than the baseline water and ZnO NF. The maximum viscosity of iron oxide was measured at a volume concentration of 0.175%, as depicted in Fig. 6. The maximum viscosity of iron oxide was measured at 0.001 N-s/m^2. The viscosities of Fe_2O_3 and ZnO NFs were experimentally measured using an Angler Viscometer and compared with the theoretical correlation equation (9). Before obtaining any results from the device, it underwent calibration. Subsequently, the results were collected. The viscosity of NFs mainly depends on volume concentration, temperature, and particle size [18]. Viscosity of Fe_2O_3 and ZnO NF decreases as the temperature of the NF increases. Their viscosity decreases as they are heated. This is attributed to the increase in the absolute temperature.

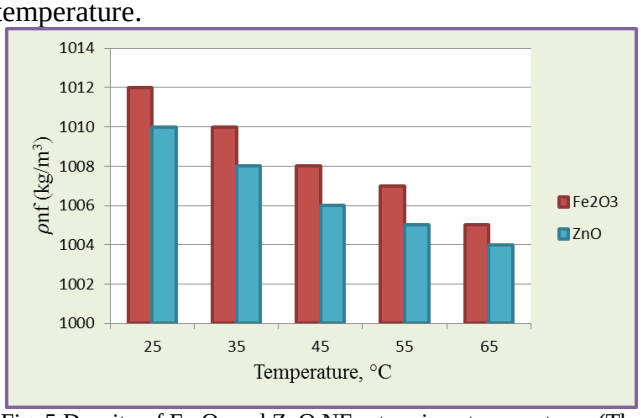

Fig. 5 Density of Fe_2O_3 and ZnO NFs at various temperatures (The authors)

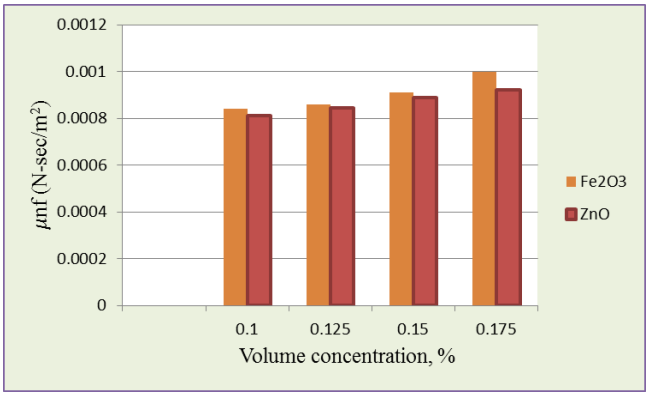

Fig. 6 Viscosity of Fe_2O_3 and ZnO NFs at various concentrations (The authors)

4.2. Thermal Conductivity of Fe_2O_3 and ZnO NFs at Various Concentrations

Various theories have shown that the thermal conductivity of NFs is greatly influenced by factors such as particle shape, size, concentration, and temperature. When Fe_2O_3 and ZnO nanoparticles are combined in the baseline water, the thermal conductivity of the NF is enhanced. This enhancement has the potential to increase the rate of heat transfer between hot and cold fluids. The random movement of nanoparticles in the baseline water increases agglomeration, which may increase the density and pumping power of the heat exchanger.

According to Fig. 7, it is evident that the thermal conductivity of the zinc oxide NF is greater than that of the iron oxide NF. This is due to the higher thermal conductivity of zinc oxide particles than iron oxide particles. The highest increase in thermal conductivity was observed in zinc oxide NF at a concentration of

0.175% by volume. This enhancement is illustrated in Fig. 7. The maximum thermal conductivity of zinc oxide is recorded as 0.71 W/m.K. The thermal conductivity of Fe_2O_3 and ZnO NFs was experimentally measured using a thermal conductivity apparatus. The results were compared with the theoretical correlation equation.

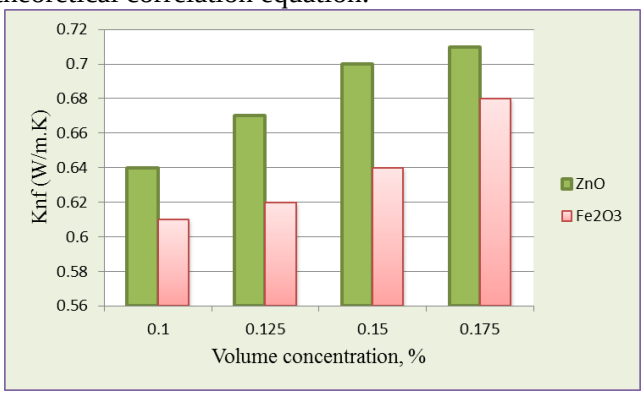

Fig. 7 Thermal conductivity of Fe_2O_3 and ZnO NF at various concentrations (The authors)

4.3. Effect of Volume Concentration on the Heat Transfer Coefficient and Friction Factor

The addition of zinc oxide and iron oxide nanoparticles to the baseline water is crucial for improving the convective heat transfer coefficient, Nusselt number, and other thermal performance parameters in parallel- and counter-flow heat exchangers. We conducted an experimental investigation to measure the thermal performance of both types of heat exchangers, involving dispersing two types of nanoparticles, Fe2O3 and ZnO, in baseline water at volume concentrations of 0.100%, 0.125%, 0.150%, and 0.175%. Forced convection heat transfer was utilized in the pipes, with the fluid flowing under a laminar flow regime facilitated by a pump. The experimental conditions used in this study were as follows:

(1) The Reynolds number of NF varied from 1600 to 3400.

(2) The temperature of the hot fluid was measured at 60°C.

(3) The mass flow rate ranged from 1 to 2 LPM, with increments of 0.25 LPM.

The impact of volume concentration on the convective heat transfer coefficient in parallel and counter flows is illustrated in Fig. 8.

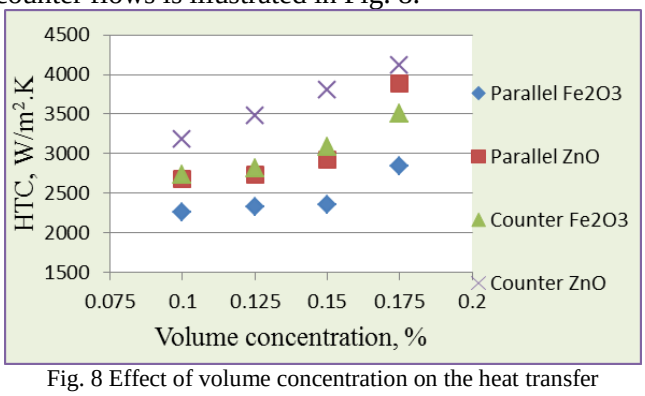

Fig. 8 Effect of volume concentration on the heat transfer coefficient in parallel and counter flows (The authors)

Fig. 8 displays the results of an experimental study on the convective heat transfer coefficient for baseline water and NF in a double-pipe heat exchanger. From Fig. 8, it is clear that the convective heat transfer coefficient increases as the volume concentration increases. The experimental results show that the suspension of nanoparticles in baseline water enhances the heat transfer coefficient. However, the enhancement was achieved because of the greater thermal conductivity of both Fe_2O_3 and ZnO NF than baseline water. A higher convective HTC was observed in the counter-flow direction than the parallel-flow direction when operating under laminar flow conditions. Based on Fig. 8, the counter-flow direction showed a higher heat transfer rate for ZnO NF than Fe_2O_3 NF. This can be attributed to the higher thermal conductivity of Fe_2O_3 NF than ZnO NF. The highest increase in convective heat transfer coefficients for Fe_2O_3 and ZnO NFs reached 3888 W/m^2.K and 4112 W/m^2.K, respectively, at a volume concentration of 0.175%. Fig. 9 illustrates the impact of the Nusselt number on NF at various flow rates across different Reynolds numbers. According to Fig. 9, the Nusselt number increases with an increase in flow rates. This is due to the higher volume concentration of nanoparticles in the base fluid and the higher thermal conductivity of both nanoparticles. Therefore, the heat transfer rate increases the Nusselt number of both water and NF. Thus, the Reynolds number of the water baseline, Fe_2O_3, and ZnO NF for the laminar flow regime ranges from 1330 to 3400. The Nusselt number range for both water and NF was observed to increase from 50 to 95. The increase in the Nusselt number was attributed to the Brownian motion and chaotic movement of the base fluid and NF within the double-pipe heat exchanger. Therefore, a higher Nusselt number is obtained at a higher Reynolds number. Fig. 9 demonstrates a strong correlation between the measured data and the results obtained from the correlation equations. This figure indicates that this study closely aligns in accuracy with the correlation established by Acharya et al. [17].

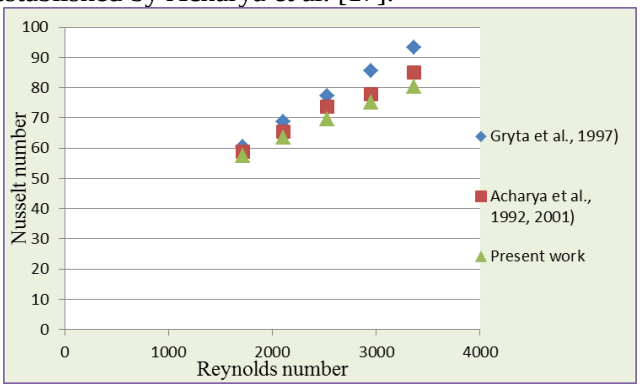

Fig. 9 Comparison of the Nusselt number obtained from calculations using the correlations developed by Gryta et al. [16] and Acharya et al. [17] (The authors)

The experimental results for the Nusselt number and friction factor using a 0.1% ZnO NF were compared with the results obtained from theoretical correlation equations. The equation proposed by Gryta et al. [16] is defined as follows:

$$Nu = 0.298Re\text{^}0.646\,Pr\text{^}0.316 \qquad (11)$$

where Re is the Reynolds number, and Pr is the Prandtl number.

The Prandtl number of NFs:

$$Pr = \frac{cp_{nf}.\mu_{nf}}{k_{nf}} \qquad (12)$$

where $cpnf$ is the specific heat of the NF in J/kg.K, μnf is dynamic viscosity of the NF in Pa.sec.

The specific heat $cpnf$ of NF is given as

$$cp\text{nf} = \phi cpp + (1-\varphi)\,cpbf \qquad (13)$$

where $cpnf, cpbf, cpp$ are specific heats of the NF, base fluid, and nanoparticle in J/Kg.K, and Ø is the percentage volume concentrations of nanoparticles.

The Acharya et al. [17] equation is defined as

$$Nu = 0.69(r/R)\text{^}0.13 * Re\text{^}0.5 * Pr\text{^}0.43 \qquad (14)$$

Filonenko's model:

$$f(th) = \ln.Re.0.790 - 1.64 \qquad (15)$$

The Blasius model:

$$f(th) = (100.Re)^{-¼} \qquad (16)$$

The friction factor is a critical component that significantly impacts the resistance and obstacles encountered by a moving fluid. This study examined the impact of different volume concentrations of Fe_2O_3 and ZnO NPs mixed in baseline water on the friction factor. The results showed that the higher densities and viscosities of the fluids led to an enhancement in the friction factor. Thus, fluid friction has significant impacts on pressure levels and the amount of power required for pumping. To reduce the agglomeration of nanoparticles, it is recommended to increase fluid motion by raising velocities and flow rates within the test section. Therefore, friction losses can be minimized by increasing the fluid's movement and motion. A higher velocity of fluid causes a higher Reynolds number but reduces the friction among fluid particles, which reduces the pumping power. The friction factor increases as the volume concentration increases and decreases as the Reynolds number increases, as shown in Fig. 10.

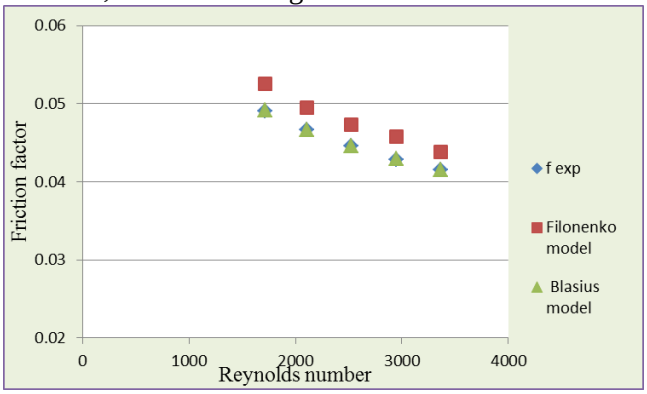

Fig. 10 Comparison of the friction factors obtained by Gryta et al. [16] and Acharya et al. [17] (The authors)

Fig. 10 illustrates the strong agreement between the experimental and theoretical results of the ZnO NF. This figure demonstrates that our research closely aligns with the Blasius model in terms of accuracy. In this study, Fe_2O_3 and ZnO NPs were mixed in baseline water to determine the effect of the volume concentration of nanoparticles, friction factor, mass flow rate, Reynolds number, and pumping power on the heat transfer coefficient. Fig. 11 demonstrates that adding 0.175% Fe_2O_3 and ZnO nanoparticles to the baseline water results in a higher friction factor than the baseline water alone. This is attributed to the higher density and viscosity of the Fe_2O_3 NF than the ZnO NF and baseline water. At a higher Reynolds number, the ZnO NFs showed a lower friction factor than Fe_2O_3 NF at a given mass flow rate.

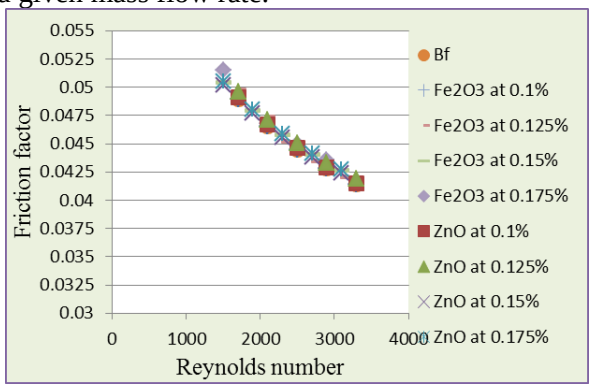

Fig. 11 Analysis of the relationship between the measured friction factor and Reynolds number (The authors)

4.4. Effect of Volume Concentration and Flow Rate on Pumping Power

Power consumption is a critical factor in energy

efficiency. If nanoparticles are added to water, the viscosity of the base fluid increases, leading to a rise in pressure drop within the test section. The increased pressure drop corresponds to the increased pumping power required for the flow per unit length. Fig. 12 illustrates the relationship between pumping power and the volume concentration of Fe_2O_3 and ZnO NFs.

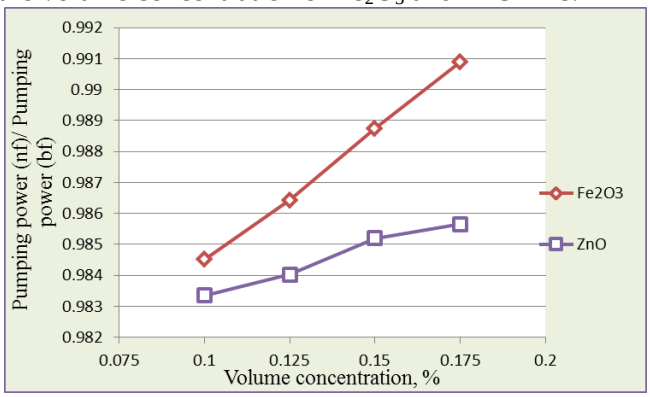

Fig. 12 Effect of volume concentration on pumping power in both flows at 1-2 LPM (The authors)

Adding 0.175% Fe_2O_3 nanoparticles to the baseline water resulted in an increase in pumping power, specifically by 5.4%, compared to the baseline water alone. This enhancement can be attributed to the higher density of the Fe_2O_3 NF than the ZnO NF and baseline water. The concept of pumping power involves the partial power consumption of the heat exchanger while it is in operation. By increasing the volume concentrations of the baseline water, pumping power can enhance consumption, leading to an increase in the heat transfer coefficient. Although the full consumption of pumping power cannot be eliminated, improvements can be made to enhance its efficiency. The pumping power of NF and base fluid ranges from 0.983 to 0.991 at volume concentrations between 0.10% and 0.175%.

As fluid velocity increases, the heat transfer rate decreases in NFs due to the sustained temperature difference caused by higher Reynolds and Nusselt numbers in the parallel- and counter-flow directions. According to Fig. 13, it is evident that increasing the flow rate of NFs at different volume concentrations results in an increase in the pumping power of both NFs in the parallel- and counter-flow directions. The increase in pumping power is a result of the higher density and viscosity of the NFs. Therefore, more friction and pressure drop are induced in both directions of NFs. Moreover, significant power is required for the mixing of Fe_2O_3 and ZnO NFs in the baseline water. The consumption of high power, measured at 0.0012 W and 0.0011 W, was observed in both Fe_2O_3 and ZnO NFs when operated at a volume flow rate of 2 LPM. According to Fig. 13, Fe_2O_3 NF consumes more power than ZnO NF due to its higher density and viscosity. It demonstrates that the efficiency of the heat exchanger improved when utilizing Fe_2O_3 and ZnO NFs at different flow rates. Moreover, a higher flow rate results in increased efficiency of the heat exchanger. Therefore, the efficiency of the counter-flow direction is greater than that of the parallel-flow direction.

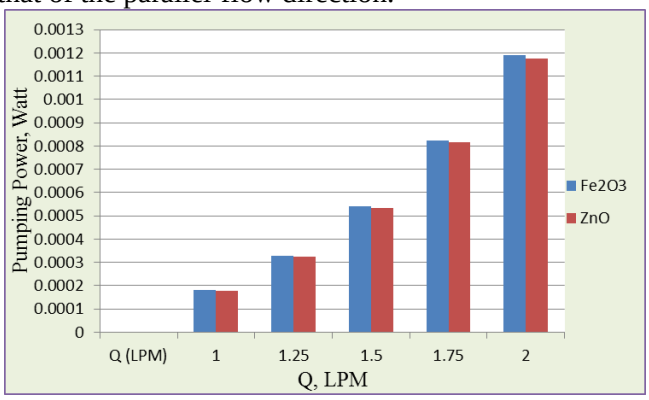

Fig. 13 Effect of NF speed on pumping power in both flows (The authors)

5. Conclusion

The experimental findings suggest that utilizing NFs containing 0.10–0.175% volume concentrations of iron oxide Fe_2O_3 and zinc oxide ZnO, at various volume flow rates, results in improved heat transfer coefficients, Nusselt numbers, friction factors, pressure drops, and pumping powers than using baseline water. This is due to the higher density and thermal conductivity of Fe_2O_3 and ZnO NFs than baseline water. The major findings of this research can be summarized as follows:

The dispersion of Fe_2O_3 and ZnO nanoparticles in the baseline water exhibited a higher density than the baseline water alone. Moreover, by utilizing Fe_2O_3 and ZnO NFs, the densities were maximally enhanced by 2.4% and 3.1%, respectively, when the particle concentration reached 0.175%, as compared to the baseline water. The average heat transfer coefficient increases as the volume concentration increases, thereby improving the thermal physical properties of the fluid. The average heat transfer coefficient for ZnO NFs showed a significant improvement, increasing from approximately 17% to 36% in both parallel- and counter-flow directions compared to iron oxide Fe_2O_3 NFs. This improvement can be attributed to the higher thermal conductivity of ZnO. Adding 0.175% Fe_2O_3 and ZnO nanoparticles to the baseline water led to a 5.2% and 3.1% increase in friction factor, respectively, as a result of the greater density of both NFs than water. Additionally, approximately 0.56%–1.1% more pumping power was consumed for ZnO and Fe_2O_3 NFs than baseline water using a 0.175% volume concentration because of the higher density and pressure drop of Fe_2O_3 NF compared to ZnO NF and baseline water. Thus, the results suggest that ZnO NF at a 0.175% volume concentration functioned very well as a working fluid for industrial requirements compared with Fe_2O_3 NFs and conventional baseline water. The primary objectives of the study were to improve heat transfer rates and experimentally analyze the pumping power consumption. This study focused

on the utilization and preparation of iron oxide and zinc oxide NFs as coolants. The NFs were tested in both types of double-pipe heat exchangers to analyze their behavior at different flow rates and operating temperatures. One of the primary criteria for selecting this study was to explore the utilization of nanoparticles in industrial applications to achieve superior results in heat transfer enhancement in both types of heat exchangers. Based on this discovery, zinc oxide outperformed iron oxide due to its superior thermal conductivity.

5.1. Comparison with Other Studies

Pumping power is a crucial factor in optimizing energy efficiency and conservation within the test rig. In previous studies, the pumping power consumption was higher compared to this research conducted using various mass flow rates with 0.2% and 0.3% volume concentrations of zinc oxide (ZnO) in the double-pipe heat exchanger.

Furthermore, Fig. 14 illustrates that this study exhibits a superior heat transfer rate of 5431 watts when the mass flow rate is 0.03 kg/s. Moreover, in the previous study, the heat transfer rate was 3941 watts at a mass flow rate of 0.029 kg/s. In the figure, blue and red bars represent this and previous works.

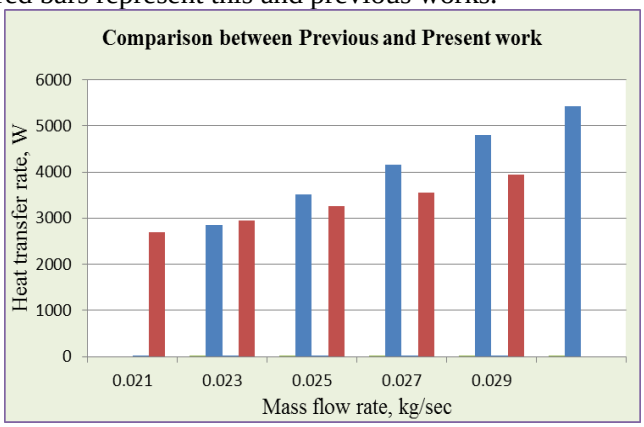

Fig. 14 Comparison of previous and this studies at 1-2 LPM (The authors)

5.2. Implications of the Study

This study also focused on NF stability and its preparation method. This study is applicable to industrial processing where hot and cold fluids exchange their maximum possible heat. Moreover, in this investigation, heat was transferred only from hot oil to cold NF, which is a novelty and main finding of this investigation that could not be found in other studies. Moreover, the Nusselt number was calculated, followed by a comparison with the correlation equation, and it was found that experimental and theoretical correlations meet their closeness values. The implications of this discovery extend to heating processing equipment, heat exchangers, power engineering devices, the chemical industry, medicine, solar collectors, and electronic devices.

5.3. Recommendations for Future Research

In the future, a hybrid nanofluid consisting of iron oxide, copper oxide, and zinc oxide may be utilized to improve heat transfer capabilities beyond the parameters explored in this study. This may enhance the thermal properties of the hybrid NF.

Nomenclature

np	nanoparticle	Re	the Reynolds number
NF	nanofluid	Th1	temperature of the hot fluid at the inlet
HX	heat exchanger	Th2	temperature of the hot fluid at the outlet
Al_2O_3	aluminum oxide	Tc1	temperature of the cold fluid at the inlet
nm	nanometer	Tc2	temperature of the cold fluid at the outlet
LPM	liters per minute	CuO	copper oxide
GPM	grams per minute		
BV	ball valve	HTC	heat transfer coefficient
GV	gate valve	Avg.	average
Wp	weight of the particle	Nu	the Nusselt number
ρbf	density of the base fluid	C_p	specific heat capacity
Fe_2O_3	iron oxide	Tw	wall temperature
ISO	International Standard	μ_{bf}	dynamic viscosity of the base fluid
VG	Organization viscosity grade		
f	friction factor	Tb	bulk temperature
h_{bf}	convective heat transfer coefficient of the base fluid	Pr	the Prandtl number
K	thermal conductivity	P nf	pressure drop of the nanofluid
℃	degree Celsius	TiO_2	titanium oxide
ZnO	zinc oxide	φ	volume concentration
Tw	wall temperature	Tb	bulk temperature

References

[1] DE CARLI M., FIORENZATO S., and ZARRELLA A. Performance of heat pumps with direct expansion in vertical ground heat exchangers in heating mode. *Energy Conversion and Management*, 2015, 95: 120-130. https://doi.org/10.1016/j.enconman.2015.01.080

[2] HATAMI M., GANJI D. D., and GORJI-BANDPY M. Experimental and numerical analysis of the optimized finned-tube heat exchanger for OM314 diesel exhaust exergy recovery. *Energy Conversion and Management*, 2015, 97: 26-41. https://doi.org/10.1016/j.enconman.2015.03.032

[3] RASHIDI M. M., & ABBASBANDY S. Analytic approximate solutions for heat transfer of a micropolar fluid through a porous medium with radiation. *Communications in Nonlinear Science and Numerical Simulation*, 2011, 16(4): 1874-1889. https://doi.org/10.1016/j.cnsns.2010.08.016

[4] KUMAR S., SHANDILYA M., CHAUHAN A., MAITHANI R., and KUMAR A. Experimental analysis of zinc oxide/water/ethylene glycol-based nanofluid in a square duct roughened with inclined ribs. *Journal of Enhanced Heat Transfer*, 2020, 27(8): 687-709. https://doi.org/10.1615/JEnhHeatTransf.2020034180

[5] GNANAVEL C., SARAVANAN R., and CHANDRASEKARAN M. Heat transfer enhancement through nano-fluids and twisted tape insert with rectangular cut on its rib in a double pipe heat exchanger. *Materials*

Today: Proceedings, 2020, 21: 865-869. https://doi.org/10.1016/j.matpr.2019.07.606
[6] LOUIS S. P., USHAK S., MILIAN Y., NEMŚ M., and NEMŚ A. Application of nanofluids in improving the performance of double-pipe heat exchangers—A critical review. *Materials*, 2022, 15(19): 6879. https://doi.org/10.3390/ma15196879
[7] NEGEED E. S. R., ALHAZMY M., ABULKHAIR H., ATTAR H. M., and HEDIA H. S. Numerical simulation of dual-tube heat exchanger equipped with an innovative turbulator containing two-phase hybrid nanofluid: Hydrodynamic and exergy analysis. *Engineering Analysis with Boundary Elements*, 2023, 155: 1059-1068. https://doi.org/10.1016/j.enganabound.2023.07.025
[8] ZHOU X., WANG Y., ZHENG K., and HUANG H. Comparison of heat transfer performance of ZnO-PG, α-Al2O3-PG, and γ-Al2O3-PG nanofluids in car radiator. *Nanomaterials and Nanotechnology*, 2019, 9. https://doi.org/10.1177/1847980419876465
[9] TENG K. H., KAZI S. N., AMIRI A., HABALI A. F., BAKAR M. A., CHEW B. T., AL-SHAMMA'A A. A., SHAW A., SOLANGI K. H., and KHAN G. Calcium carbonate fouling on double-pipe heat exchanger with different heat exchanging surfaces. *Powder Technology*, 2017, 315: 216-226. https://doi.org/10.1016/j.powtec.2017.03.057
[10] SHARMA H. K., VERMA S. K., SINGH P. K., KUMAR S., PASWAN M. K., and SINGHAL P. Performance analysis of paraffin wax as PCM by using hybrid zinc-cobalt-iron oxide nano-fluid on latent heat energy storage system. *Materials Today: Proceedings*, 2020, 26: 1461-1464. https://doi.org/10.1016/j.matpr.2020.02.300
[11] SHEIKHOLESLAMI M., GORJI-BANDPY M., and GANJI D. D. Fluid flow and heat transfer in an air-to-water double-pipe heat exchanger. *The European Physical Journal Plus*, 2015, 130: 225. https://doi.org/10.1140/epjp/i2015-15225-y
[12] GORMAN J. M., KRAUTBAUER K. R., and SPARROW E. M. Thermal and fluid flow first-principles numerical design of an enhanced double pipe heat exchanger. *Applied Thermal Engineering*, 2016, 107: 194-206. https://doi.org/10.1016/j.applthermaleng.2016.06.134
[13] AGHAYARI R., JAHANIZADEH S., ARANI J. B., MADDAH H., POURALI M., and KHALAJ A. H. Heat Transfer of Iron Oxide Nanofluid in a Double Pipe Heat Exchanger. *Journal of Materials Science & Surface Engineering*, 2015, 2(1): 84-89. https://www.jmsse.in/files/211reza%20aghayari%20et%20al.pdf
[14] ZHANG Y., HANGI M., WANG X., and RAHBARI A. A comparative evaluation of double-pipe heat exchangers with enhanced mixing. *Applied Thermal Engineering*, 2023, 230: 120793. https://doi.org/10.1016/j.applthermaleng.2023.120793
[15] ÖZENBINER Ö., & YURDDAŞ A. Numerical analysis of heat transfer of a nanofluid counter-flow heat exchanger. *International Communications in Heat and Mass Transfer*, 2022, 137: 106306. https://doi.org/10.1016/j.icheatmasstransfer.2022.106306
[16] LI H., WANG Y., HAN Y., LI W., YANG L., GUO J., LIU Y., ZHANG J., ZHANG M., and JIANG F. A comprehensive review of heat transfer enhancement and flow characteristics in the concentric pipe heat exchanger. *Powder Technology*, 2022, 397: 117037. https://doi.org/10.1016/j.powtec.2021.117037
[17] DANDOUTIYA B. K., & KUMAR A. Experimental analysis of thermal performance factor for double pipe heat exchanger with ZnO–water nanofluid. *Proceedings of the Institution of Mechanical Engineers, Part E: Journal of Process Mechanical Engineering*, 2023. https://doi.org/10.52716/jprs.v13i2.687
[18] AGHAYARI R., MADDAH H., BAGHBANI ARANI J., MOHAMMADIUN H., and NIKPANJE E. An Experimental Investigation of Heat Transfer of Fe_2O_3/Water Nanofluid in a Double Pipe Heat Exchanger. *International Journal of Nano Dimension*, 2015, 6(5 (Special Issue for NCNC)): 517-524. https://sid.ir/paper/322284/en
[19] DHAHRI M., AOUINET H., and SAMMOUDA H. A new empirical correlating equation for calculating effective viscosity of nanofluids. *Heat Transfer—Asian Research*, 2019, 48(5): 1547-1562. https://doi.org/10.1002/htj.21445

参考文:

[1] DE CARLI M.、FIORENZATO S. 和 ZARRELLA A. 垂直地热交换器中直接膨胀热泵在加热模式下的性能。能源转换与管理，2015年，第95期：120-130。https://doi.org/10.1016/j.enconman.2015.01.080
[2] HATAMI M.、GANJI D. D. 和 GORJI-BANDPY M. 针对奥姆314柴油机尾气能量回收的优化翅片管热交换器的实验和数值分析。能源转换与管理，2015年，第97期：26-41。https://doi.org/10.1016/j.enconman.2015.03.032
[3] RASHIDI M. M., & ABBASBANDY S. 微极性流体通过辐射多孔介质传热的解析近似解。非线性科学与数值模拟通讯，2011，16(4)：1874-1889。https://doi.org/10.1016/j.cnsns.2010.08.016
[4] KUMAR S.、SHANDILYA M.、CHAUHAN A.、MAITHANI R. 和 KUMAR A. 对倾斜肋条粗糙方形管道中氧化锌/水/乙二醇基纳米流体的实验分析。增强传热杂志，2020，27(8)：687-709。https://doi.org/10.1615/JEnhHeatTransf.2020034180
[5] GNANAVEL C.、SARAVANAN R. 和 CHANDRASEKARAN M. 通过纳米流体和肋片上有矩形切口的扭带插入物在双管热交换器中增强传热。当今材料：论文集，2020，21：865-869。https://doi.org/10.1016/j.matpr.2019.07.606
[6] LOUIS S. P.、USHAK S.、MILIAN Y.、NEMŚ M. 和 NEMŚ A. 纳米流体在提高双管热交换器性能中的应用——评论。材料，2022，15(19)：6879。https://doi.org/10.3390/ma15196879
[7] NEGEED E. S. R.、ALHAZMY M.、ABULKHAIR H.、ATTAR H. M. 和 HEDIA H. S. 配备创新湍流器的双管热交换器的数值模拟，该湍流器包含两相混合纳米流体：流体动力学和火用分析。边界元工程分析，2023，155：1059-1068。https://doi.org/10.1016/j.enganabound.2023.07.025
[8] 周晓玲，王燕，郑凯，黄华。氧化锌、α-氧化铝-前列腺素、γ-氧化铝-前列腺素纳米流体在汽车散热器中的传热性能比较。纳米材料与纳米技术，2019，9。https://doi.org/10.1177/1847980419876465

[9] TENG K. H.、KAZI S. N.、AMIRI A.、HABALI A. F.、BAKAR M. A.、CHEW B. T.、AL-SHAMMA'A A. A.、SHAW A.、SOLANGI K. H. 和 KHAN G. 具有不同热交换表面的双管热交换器上的碳酸钙污垢。粉体技术，2017，315：216-226。https://doi.org/10.1016/j.powtec.2017.03.057

[10] SHARMA H. K.、VERMA S. K.、SINGH P. K.、KUMAR S.、PASWAN M. K. 和 SINGHAL P. 混合锌钴铁氧化物纳米流体在潜热储能系统中对石蜡作为相控阵相机的性能分析。当今材料：论文集，2020，26：1461-1464。https://doi.org/10.1016/j.matpr.2020.02.300

[11] SHEIKHOLESLAMI M.、GORJI-BANDPY M. 和 GANJI D. D. 空气-水双管热交换器中的流体流动和传热。欧洲物理杂志加，2015年，130：225。https://doi.org/10.1140/epjp/i2015-15225-y

[12] GORMAN J. M.、KRAUTBAUER K. R. 和 SPARROW E. M. 增强型双管热交换器的热和流体流动第一性原理数值设计。应用热工程，2016年，107：194-206。https://doi.org/10.1016/j.applthermaleng.2016.06.134

[13] AGHAYARI R.、JAHANIZADEH S.、ARANI J. B.、MADDAH H.、POOURALI M. 和 KHALAJ A. H. 双管热交换器中氧化铁纳米流体的传热。材料科学与表面工程杂志，2015，2（1）：84-89。https://www.jmsse.in/files/211reza%20aghayari%20et%20al.pdf

[14] ZHANG Y.、HANGI M.、WANG X. 和 RAHBARI A. 增强混合双管换热器的比较评估。应用热工程，2023，230：120793。https://doi.org/10.1016/j.applthermaleng.2023.120793

[15] ÖZENBINER Ö. 和 YURDDAŞ A. 纳米流体逆流换热器传热的数值分析。国际传热传质通讯，2022年，137：106306。https://doi.org/10.1016/j.icheatmasstransfer.2022.106306

[16]李华、王燕、韩燕、李伟、杨琳、郭江、刘燕、张建、张明、姜锋。同心管换热器传热强化和流动特性综合综述。粉体技术，2022年，397：117037。https://doi.org/10.1016/j.powtec.2021.117037

[17] DANDOUTIYA BK 和 KUMAR A。氧化锌-水纳米流体双管换热器热性能因子实验分析。机械工程师学会会刊，埃部分：过程机械工程杂志，2023年。https://doi.org/10.52716/jprs.v13i2.687

[18] AGHAYARI R.、MADDAH H.、BAGHBANI ARANI J.、MOHAMMADIUN H. 和 NIKPANJE E. 双管热交换器中氧化铁/水纳米流体传热的实验研究。国际纳米维度杂志，2015年，6(5（全国数控协会特刊）)：517-524。https://sid.ir/paper/322284/en

[19] DHAHRI M.、AOUINET H. 和 SAMMOUDA H. 一种用于计算纳米流体有效粘度的新型经验关联方程。《传热—亚洲研究》，2019年，48(5): 1547-1562。https://doi.org/10.1002/htj.21445